DOI 10.1007/s10553-022-01449-6
Chemistry and Technology of Fuels and Oils, Vol. 58, No.5, November, 2022 (Russian Original No.5, September–October, 2022)

INNOVATIVE TECHNOLOGIES OF OIL AND GAS

LASER RAMAN SPECTROSCOPY – AN EFFECTIVE METHOD FOR TOTAL PROCESS CONTROL OF POLY-α-OLEFIN OIL PRODUCTION

A. Kh. Kuptsov✉, E. V. Zhmaeva, A. V. Kulik, K. B. Rudyak

The developed approaches to increasing the analytical selectivity by laser Raman spectroscopy and the use of chemometrics and a proprietary algorithm for self-tuning calibration models with the efficiency and speed of the method have shown a rare and excellent opportunity for informationally equivalent on-line control of all technological stages of the production of poly-α-olefin oils and other products through a network of fiber-optic probes. Oligomers of C_6, C_8, and C_{10} α-olefins obtained by heterogeneous chromium-oxide catalysis technology developed at LLC «RN-RD CENTER», as shown by the Raman spectra, differ from analogs obtained by homogeneous synthesis by the variety of unsaturated group structures and a greater width and variability of the molecular-mass distribution, which makes it possible to regulate a wide assortment of low- and high-molecular-mass products. A special case – the atypically high sensitivity of Raman spectra to the chain length – makes it possible during the synthesis to predict and adjust in real time the molecular mass of the oligomers and other target properties and to replace a fleet of traditional analytical equipment with one method.

Keywords: laser Raman spectroscopy, self-tuning model, process control, α-olefins, oligomerization, synthetic base oil stocks.

Laser Raman spectroscopy combines the advantages of the information value of the fundamental modes in classical mid-IR spectroscopy and of the response and rheology of flow analysis probes and the transparency of fiber optics in near-IR (NIR) spectroscopy. Rapid development of Raman scattering technologies has been reported and is predicted in analytical reviews of process control methods [1, 2] because of the progress achieved on technical improvements and background minimization. The advantages of the efficiency and speed of Raman spectroscopy as compared to other analytical methods, particularly the use of a proprietary algorithm for self-tuning calibration models, were recently shown using control of a process involving olefinic hydrocarbons [3-5].

Separation of target low- (particularly dimers) and high-molecular-mass synthetic poly-α-olefins has become necessary because of the tightening of various operational requirements for them. For this, expensive modular solutions using specialized dual homogeneous catalytic systems to give narrow molecular-mass distributions of the corresponding products are often used [6]. A more economical solution using a single heterogeneous catalyst with wide variations of the synthesis conditions and technologically

LLC «RN-RD CENTER», Moscow. *Corresponding author: A. Kh. Kuptsov✉. E-mail: KuptsovAK@rdc.rosneft.ru.*
Translated from *Khimiya i Tekhnologiya Topliv i Masel*, No. 5, pp. 45–51 September–October, 2022.

regulated yields of products with different molecular masses began to be investigated. Features of the technological conditions and process scheme, the physicochemical properties of the obtained products, and the advantage of this technology for industrial manufacturing were compared with analogs [7].

Improvement of control methods at each stage assumed special significance in this approach to more effective and economical monitoring and control of manufacturing processes. The previous work showed that the fleet of equipment necessary for total control of a multi-stage technological cycle included various gas and gel-permeation chromatographs, a NIR spectrometer, and several physicochemical analyzers [7]. The possibility of adequately (by speed, equivalence, and cost effectiveness) replacing them by a single Raman spectrometer with a multiplexer and a network of fiber-optic probes in the input and output streams was studied in the present work as an alternative to the traditional complex of labor- and time-consuming methods. It is noteworthy that the control scheme could possibly be even further simplified by using fast superconducting nanowire single-photon detector with picosecond lasers. This would allow Raman spectra to be recorded without spectrometers (on instruments without dispersive elements) because of the dispersion of the phase velocities of various wavelengths within the optical fibers themselves [8].

Poly-α-olefins (α-hexene, α-octene, α-decene) were synthesized over heterogeneous chromium-oxide catalysts using the RN-RDC method. Reaction mixtures with monomers, their fractions, and their hydrogenation products were studied by Raman spectroscopy at all stages of the technological cycle.

Raman spectra were recorded using a DXR spectrometer (Thermo Nicolet, USA) with excitation by a laser at 780 nm, a diffraction grating of 1800 g/mm, input slit widths of 25 and 50 μm, and spectral resolution 2-5 cm^{-1}. An RPL780/12-5 retro-scattering probe with a focal length of 5 mm and a numerical aperture of 0.4 and a 5-m fiber-optic cable were used for remote recording. The total time to measure a spectrum was <5 min. Calibration curves were constructed from gel-permeation chromatographic data and gravimetric analyses.

A structured band of C=C stretching vibrations with two low-frequency shoulders in the range 1710-1610 cm^{-1} was deconvoluted into three components. First, background was subtracted from the linearized band. Raman spectra were approximated as a convolution of Gaussian and Lorentzian functions. Parameters of component bands were fitted using optimization programs in the OMNIC™ application package embedded in the Thermo-Nicolet spectrometer. Chemometric models were developed using Turbo Quant (TQ) Analyst 9 software.

Modern manufacturing of various grades of synthetic oils is usually a multi-stage process including conversion in a reactor of an α-olefin monomer (usually α-hexene, α-octene, or α-decene) into oligomers; separation at the outlet of the synthesis reactor of unreacted monomer; isolation of dimer fractions; separation of oligomers in fractionating columns into two or three commercial fractions; and hydrogenation of unsaturated groups (stabilization of the commercial product) [9]. **Figure 1** shows a conceptual

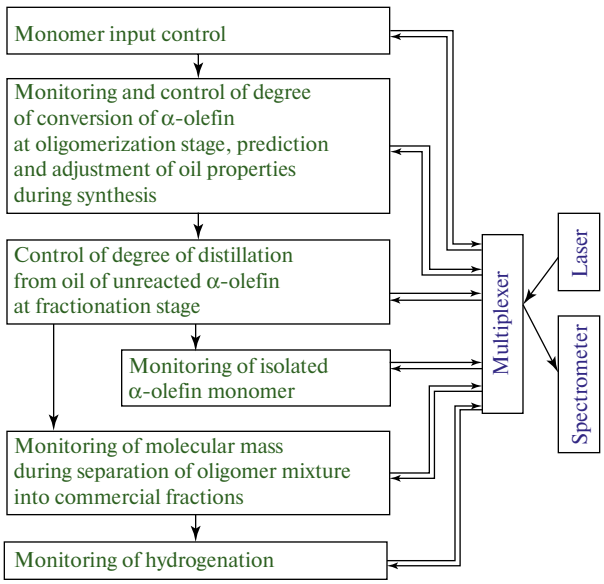

Fig. 1. Conceptual diagram of Raman spectroscopic monitoring system on processing line for production of poly-α-olefin oils through a network of fiber-optic probes

diagram of the sequence of technological stages monitored by Raman spectroscopy in the production of poly-α-olefin oils.

The first control point of the purity of the starting α-olefin monomers (and purified unreacted used monomers for recycling) is arbitrarily situated at the inlet of the synthesis reactor although it could be arbitrarily placed close to the unloading site of the entering monomer. The degree of conversion of the α-olefin into oligomers is monitored from the fraction of unreacted monomer at the second point situated at the synthesis reactor outlet. The properties of the oils can be predicted and subsequently adjusted during the synthesis by using the relative intensity of C=C stretching vibrations and oligomer skeletal-vibration bands. The target properties are determined using calibration chemometric models developed beforehand using chromatographic data and physicochemical methods (molecular composition of monomer and dimer fractions, average molecular mass of oligomer fractions, viscosity, density, iodine/bromine number, etc.). The third control point is installed in the oligomer stream after separating unreacted monomer by fractionation. The separated monomer fraction is also analyzed by Raman spectroscopy to determine its purity and the feasibility of recycling or designation of it for other purposes. The average molecular masses of fractions are also monitored using Raman spectra at outlets from the fractionation column after separation of the oligomer mixture into dimers and heavy oily and intermediate commercial fractions. Spectral monitoring is also used in the final hydrogenation stage of the oily fraction (and other fractions if necessary).

The present work studied samples obtained via synthesis over a heterogeneous chromium-containing catalyst. Standard FT Raman and FTIR spectra of various poly-α-olefins and ethylene copolymers with α-olefins have been published [10]. Poly-α-olefins have been studied using various methods [11-15]. However, data demonstrating that the degree of conversion can be monitored were not given. Although such problems are not typical of spectral methods, they have several favorable features for solving them by Raman spectroscopy. Only one C=C bond is always present in the obtained oligomer for any degree of conversion. Therefore, the intensity ratio of bands of saturated and unsaturated groups correlates with the mass increase of the oligomer. Also, Raman spectra are especially sensitive for detecting C=C bonds because of the very high polarizability of unsaturated groups.

It is noteworthy that, according to the previous work [11-15], products obtained from structural transformations during oligomerization of α-olefins (**Table 1**) are dominated before hydrogenation by vinylidene-type unsaturation. The positions of their C=C stretching vibration maxima (1651-1645 cm^{-1}) are very similar to those of the α-olefin monomers (1645-1640 cm^{-1}). Overlap of their band contours complicates quantitative monitoring of the conversion. According to NMR data [11], unsaturated vinylidene-type $R_1R_2C{=}CH_2$ groups (with a decrease from 85 to 76% in the order C_5–C_{10}) and trisubstituted $R_1R_2C{=}CHR_3$ groups (with an increase from 12 to 18% in the order C_5–C_{10}) were observed to form primarily in poly-α-olefins obtained from C_5, C_6, C_8, and C_{10} monomers by homogeneous catalysis. The content of vinylene-type unsaturated groups was insignificant (increasing

Table 1

Catalyst type	Monomer	Dimer	Oligomer	Hydrogenated oligomer
Homogeneous	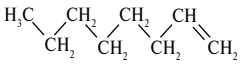	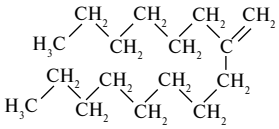	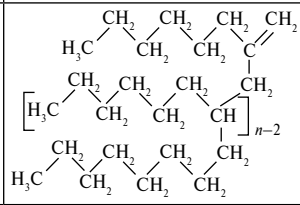	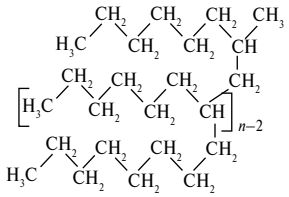
Heterogeneous chromium-oxide	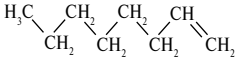	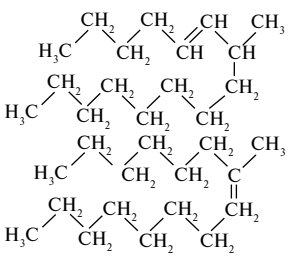	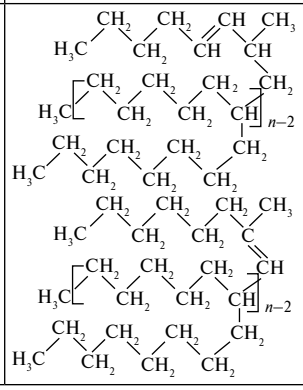	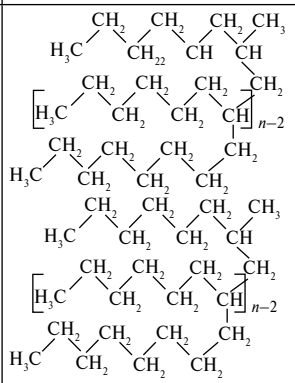

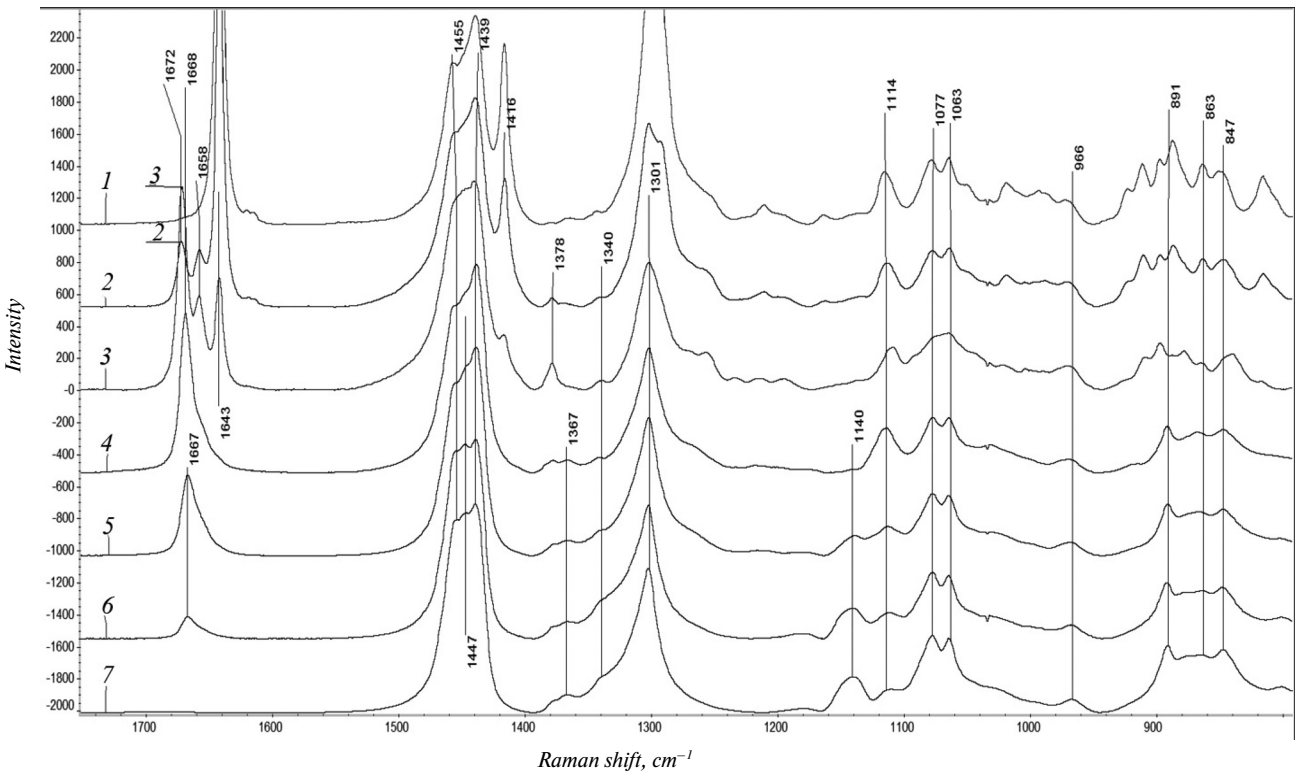

Fig. 2. Raman spectra scaled to band at 1439 cm^{-1}: starting α-octene monomer (1); distillate from reaction mixture of monomer fraction of different batches (2, 3); dimer fraction (4); oligomer fraction (5), vat residue oligomers (6), vat residue hydrogenated oligomers (7)

from 2 to 5% in the order C_5–C_{10}).

Advantageous features of the structures of the poly-α-olefins synthesized by us over heterogeneous chromium-oxide catalysts were the dominance of internal vinylene C=C bonds in *trans*- and *cis*-configurations, trisubstituted structures with lower contents of vinylidene unsaturation (which was confirmed by IR and NMR spectroscopic data), and the resulting substantial high-frequency shift of C=C Raman stretching bands of the oligomers from the monomer band. It is noteworthy that all poly-α-olefins obtained over the various catalysts acquired analogous structures after hydrogenation.

Figure 2 shows typical Raman spectra for all main stages of the technological manufacturing cycle of the poly-α-olefin oils. Spectral differences of the unsaturated groups of the monomers and oligomers can be seen.

The dimer had an unbranched structure with a methyl substituent in the 7-position while the oligomers were characterized by branched comb-like structures. Therefore, skeletal vibrations of the dimers and oligomers had several differences in the range of C–C stretching vibrations with a loss of intensity and a shift of the maximum from 1114 to 1109 cm^{-1} and an increase of intensity for the band at 1140 cm^{-1} as the molecular mass increased. Shifts of skeletal vibrational bands were also reported in spectra of the hydrogenated oligomers [12-15]. This was especially notable up to pentamers. Therefore, the increased width of the molecular-mass distribution in the wider fractions correlated with the broadening of the bands of C–C symmetric stretching vibrations. Although the most noticeable differences were observed for the stronger C=C stretching vibrations of dimers as compared to oligomers, the calibration chemometric model could be developed from the range of skeletal vibrations if it was necessary to estimate the average molecular mass, the width of its distribution, or the content of dimers in the low-molecular-mass oligomer fraction.

The assignments of Raman bands given previously [11] need to be corrected. Considering that bands in previous studies [12-15] were assigned only for hydrogenated samples without unsaturated groups, the assignments of Raman bands of the unsaturated oligomers are given by us in **Table 2**.

Table 2

Position of maximum, cm^{-1}	Proposed assignment
1667–1672	Superposition of ν_s(C=C) in trans $R_1HC=CHR_2$ (low-frequency 1667 cm–1) and groups of trisubstituted $R_1(CH_3)C=CHR_2$ and trans-β unsaturation (high-frequency 1672 cm^{-1} part of the band)
1657	Superposition of ν_s(C=C) in cis $R_1HC=CHR_2$ and in vinylidene $R_1R_2C=CH_2$ (low-frequency part of the shoulder)
1641	ν_s(C=C) in $R_1HC=CH_2$ of monomers
1455 1447, 1439	Superposition of $\delta(CH_3)$, $\delta(CH_2)$ and Fermi-resonance doublets $\delta_s(CH_2)$ with $\gamma(CH_2)_n$ overtones
1435–1410	Superposition of ($\delta_s(CH_2)$)+ δ(=CH)) in monomers and dimers
1416	$\delta_\omega(=CH_2)$ in $R_1HC=CH_2$ of monomers
1378	$\delta(CH_3)$ in $R_1(CH_3)C=CHR_2$ (strong) and terminal groups (weak)
1365	$\delta(CH_3)$ of terminal groups
1301	Superposition of $\delta(CH_2)$ in trans and gauche conformers (high-frequency part)
1141	ν_s(C-C) in trans chain segments (frequency sensitive to degree of polymerization)
1109	Superposition of ν_s(C–C) и (ν_s(C–C)+δ(=CH)) conjugated with C=C bonds
1077	ν_{as}(C-C) of gauche conformers
1063	ν_{as}(C-C) of trans conformers
891	ν_{as}(C-C) of trans-trans conformers of terminal $-(CH_2)_4-CH_3$ segments
870	ν_{as}(C-C) of trans-gauche conformers of terminal $-(CH_2)_4-CH_3$ segments
863	ν_{as}(C-C) of gauche-gauche conformers of terminal $-(CH_2)_4-CH_3$ segments
847	ν_{as}(C-C)) of gauche-trans conformers of terminal $-(CH_2)_4-CH_3$ segments
N o t e . ν_s and ν_{as} are symmetric and antisymmetric stretching vibrations, δ – bending, δ_s – scissoring, δ_t – twisting, δ_ω – wagging, δ_γ – rocking.	

Impurities contained in the α-olefin monomer did not undergo polymerization, accumulated during the synthesis, and were fractionated with the monomer as “fraction 1.” Further concentration of the impurities facilitated their identification during an evaluation of the purity of the added starting monomer.

Figure 2 (lines 1-3) shows Raman spectra of starting α-octene and different batches of the monomer fraction that are denoted further as fractions 1–1 and 1–2, which were enriched to different degrees with the impurities. These fractions contained α-octene and β-, γ-, and δ-octenes with internal unsaturation. Their accumulation could often promote side catalytic migration of the monomer unsaturation from the α- to the β-position. Differences in the impurity contents relative to α-octene in fractions 1–1 and 1–2 determined the feasibility of recycling the monomer or designating these fractions for other commercial purposes. Figure 2 shows that the intensity of the α-octene C=C stretching band near 1641 cm^{-1} in Raman spectra of fractions 1–1 and 1–2 was greater than that of C=C stretching vibrations of the impurities with bands at 1672 and 1657 cm^{-1} (due to *trans*- and *cis*-configurations of β- and γ-octenes). This could indicate that recycling of samples of fraction 1–1 was advisable while olefins of fraction 1–2 could have a different commercial value.

The positions of the C=C stretching maxima of fractions 1–1 and 1–2 were shifted to higher frequencies as compared to Raman spectra of the unsaturated structures in subsequent stages. This together with the very high relative intensity of the band at 1378 cm^{-1} (typical of CH_3 groups conjugated to a C=C bond) was indicative of a high β-octene content. The possibility of estimating the contributions of the two types of components (*trans*-β- and *trans*-γ-olefins) to the spectrally unresolved high-frequency band of C=C stretching vibrations was previously studied by us [4, 5]. A self-tuning calibration model and a formula for estimating the fractional contribution of *trans*-β C=C structures (and trisubstituted unsaturation in dimers and oligomers) to the high-frequency peak at 1672 cm^{-1} overlapped with *trans*-vinylene (*trans*-γ) C=C structures were investigated earlier by us [4, 5]. The selectivity of Raman spectroscopy could be improved over the information value of chromatography if the previously obtained formula was used.

Figure 2 clearly shows the various well-resolved spectral changes in the range of C=C and C–C stretching bands of the oligomers relative to the intensities of scissoring, twisting, and other bands of saturated groups as the molecular mass of the oligomers increased. This favorably differentiated the information value of the Raman spectra from the spectra given before [11-15] (and from NIR spectra) and allowed all stages of the technological cycle to be monitored by a single method (Fig. 1). The recording time of the Raman spectra was 100-300 s, which allowed processes along the whole technological line at a radius up

to 200-300 m from the spectrometer situated within a shelter (or another room) in the middle half-kilometer of the industrial site to be monitored in <30 min through fiber-optic cables. The total time was less than the limiting time in several chromatographic and physicochemical analyzers (even without considering the time for taking samples and delivering them to these analyzers) operating in parallel.

The fraction of unreacted monomer relative to the initial amount of monomer and; correspondingly, the fraction of monomer in the oligomer mixture at the reactor outlet had to be determined to find the degree of conversion into the oligomer. Two different calibration models of the dependences of the residual α-octene content in the mixture of octene oligomers were constructed to monitor the residual content of unreacted monomer in the oligomer stream at the reactor outlet and the fractionation-column outlet after distillation of the monomer. The first model did not require linearization of the baseline express model for monomer concentrations of 100-5% at the synthesis reactor outlet and was more convenient for commissioning and startup tests of the synthesis reactor upon loading new monomers. Also, this model clearly indicated the average molecular mass of the oligomers for predicting and adjusting the ratio of high- and low-molecular-mass products and their properties.

The first and second parameters could be determined as the amplitude ratio between the intensity maximum and minimum of the first derivative of the monomer C=C stretching band at 1641 cm^{-1} ($I_{1639} - I_{1644}$) and the internal C=C band at 1667 cm^{-1} ($I_{1663} - I_{1672}$) to the amplitudes between the intensity maximum and minimum of the first derivative of $CH_{2,3}$ bending vibrations at 1440 or 1300 cm^{-1}. A partial least-squares (PLS) model was calibrated and optimized for Raman spectra measured at variable sample temperatures of 15-55ºC, which corresponded to the reactor outlet temperature after the chiller. Thus, the root-mean-square error of calibration (RMSEC) according to residual monomers for ten calibration samples was 0.296 (correlation coefficient 0.9999). The root-mean-square error of prediction (RMSEP) for seven check samples was 0.403 (correlation coefficient 0.9998). A separate calibration was performed for the working range of typical residual monomer of 1-20%. An RMSEP of 0.179 was reached for a broad temperature range. An RMSEP of 0.11 was achieved in a series of measurements limited by ambient temperatures (thermostatted samples under industrial conditions in bypasses in a narrower temperature range of ±3º were required for this).

A separate model in the range from 0.25 to 11 wt% was built for low concentrations of residual α-octene monomer in the oligomer stream after its distillation in the fractionating column. A correction was made for the interfering background of internal C=C stretching vibrations to increase the accuracy at low concentrations. For this, three components at 1668, 1657, and 1641 cm^{-1} were obtained by deconvolution of the contour. Then, the summed spectrum of the first two was automatically normalized and subtracted from the measured spectra to construct the correct baseline of the monomer band.

The optimal functions were produced by a PLS method from a calibration set of spectra from eight samples over a broad temperature range. The RMSEC was 0.12 with a correlation coefficient of 0.9993. An independent set of seven test samples gave a calculated RMSEP of 0.134 with a correlation coefficient of 0.9986. The relative error in the middle calibration range was <2.2%. An RMSEP of 0.076 (relative error of ~1.3%) with a correlation coefficient of 0.9991 was attained for thermostatted samples at at temperature variations of ±3º. The first two models of Raman scattering were slightly inferior to the NIR method (2.2% vs. 2.0%) because of the higher photometric accuracy of the latter. However, the Raman scattering model at low monomer concentrations was more accurate (0.076% vs. 0.157%) and had a higher detection limit.

Hydrogenated samples exhibited an experimentally observed hyperbolic dependence of the degree of oligomerization *n* only in the range from 1 to 5 according to shifts of C–C stretching vibrations and low-frequency transverse acoustic modes <250 cm^{-1} [12-15]. The shifts of rather broad bands were obscured by experimental error at higher degrees of polymerization. The intensity of C=C bands with maxima at ~1667 cm^{-1} relative to strong unsaturated C–H bending bands near 1440 and 1300 cm^{-1} was a sensitive tool for unsaturated samples obtained via heterogeneous chromium-oxide catalysis. The rather strong band near 1300 cm^{-1} turned out to be more convenient because of the complicated contour of the first band, which was sensitive to Fermi-resonance couplings with other modes and shape changes upon decreasing the contribution of unsaturated groups in the range 1430-1390 cm^{-1}, considering previous experimental data and calculations [16, 17]. TThe model was developed using the dependence of the intensity ratio I_{1667}/I_{1300} on the quantity $1000/MM_{av}$, where the average molecular mass MM_{av} was obtained by gel-permeation chromatography. In this instance, Raman scattering turned out to be much more sensitive than the NIR method for determining MM_{av} (the correlation coefficients for NIR spectra were <0.6). The accuracy of the model from Raman spectra included *a priori*

the error of the reference gel-permeation chromatography method. Therefore, it was slightly less than the accuracy of the latter. However, the rapidity and accuracy of the Raman spectroscopic monitoring method was entirely adequate for quick regulation of the synthesis conditions to tune to given yields of various commercial fractions of given molecular masses.

The effect of temperature variations on spectra of the poly-α-olefins within the limits of climatic variations was modeled on a spectral thermal apparatus [18].

The NIR method was insensitive to residual unsaturation to control the hydrogenation time as compared to the Raman spectroscopic method. The iodine number according to GOST 2070–82 is the standard method for determining unsaturation in oil products. The relative accuracy of method A was 10%; of method B for lower concentrations ($X < 1$), 15%. The detection limits by the standard method were hundredths of the iodine number. The Raman spectroscopic method could detect residual unsaturation to thousandths of an iodine number and could optimize the hydrogenation time according to the standard detection threshold of residual unsaturation on the iodine scale.

Thus, the studies found that the accuracy of the Raman method was comparable to alternative methods in a series of six main types of control. Unification of the analysis provided equal rapidity and accuracy over the whole technological line and lacked limiting steps, which was convenient for process control. The method was much more cost effective than the alternative version of a required fleet of technical instruments for control by traditional methods. The total time for sequential query of all system probes was less than the limiting time of traditional analyzers operating in parallel. Considering that time was not spent on collecting and delivering analytical samples, the regulation and optimization of technological processes in real time was considerably faster.

REFERENCES

1. Process Spectroscopy Market (Technology Types - Near infrared (NIR) spectroscopy, Raman spectroscopy and Fourier Transform infrared (FTIR) spectroscopy) - Global Industry Analysis, Size, Share, Growth, Trends and Forecast 2019–2027. http://www.transparencymarketresearch.com/process-spectroscopy-market.html (accessed May 21, 2021).
2. K. A. Esmonde-White, M. Cuellar, C. Uerpmann, et al., *Anal. Bioanal. Chem.*, **409**, No. 3, 637-649 (2017).
3. A. Kh. Kuptsov, O. G. Karchevskaya, T. E. Kron, et al., *Neft. Khoz.*, No. 10, 125-127 (2016).
4. A. Kh. Kuptsov, T. E. Kron, O. G. Karchevskaya, et al., RU Pat. 2,581,191, Apr. 20, 2016, "Method of determining content of olefin s in synthetic liquid hydrocarbons obtained via Fischer Tropsch method (versions)."
5. A. Kh. Kuptsov, O. G. Karchevskaya, G. A. Korneeva, et al., *Zh. Prikl. Spektrosk.*, **86**, No. 2, 290-297 (2019).
6. Q. Yang, T. R. Crain, J. T. Lanier, et al., US Pat. 8,940,842, Jan. 27, 2015, "Method for controlling dual catalyst olefin polymerizations."
7. A. Kh. Kuptsov, I. A. Arutyunov, L. A. Khakhin, et al., *Khim. Tekhnol. Topl. Masel*, No. 2, 35-39 (2020).
8. J. Toussaint, S. Dochow, I. Latka, et al., *Opt. Express*, **23**, No. 4, 5078-5090 (2015).
9. S. Reid-Peters, "Group IV base stocks–PAO," UTS Seminar, ExxonMobil Chemical, XP055260987, Sept. 13-15, 2011, pp. 1-27.
10. A. Kh. Kuptsov and G. N. Zhizhin, Fourier-transform Raman and Fourier-transform IR Spectra of Polymers [in Russian], Tekhnosfera, Moscow, 2013, 696 pp.
11. I. Kim, J.-M. Zhou, and H. Chung, *J. Polym. Sci., Part A: Polym. Chem.*, **38**, 1687-1697 (2000).
12. Yu. V. Zavgorodnev, K. A. Prokhorov, G. Yu. Nikolaeva, et al., *Laser Phys.*, No. 23, 025701 (2013).
13. E. A. Sagitova, P. Donfack, G. Yu. Nikolaeva, et al., *Vib. Spectrosc.*, No. 84, 139-145 (2016).
14. I. E. Nifant′ev, A. A. Vinogradov, A. A. Vinogradov, et al., *Appl. Catal., A*, **549**, 40-50 (2018).
15. E. A. Sagitova, G. Yu. Nikolaeva, K. A. Prokhorov, et al., *Laser Phys.*, No. 29, 015701 (2019).
16. S. Abbate, G. Zerbi, and S. L. Wunder, *J. Phys. Chem.*, **86**, No. 16, 3140-3149 (1982).
17. S. M. Kuznetsov, V. S. Novikov, E. A. Sagitova, et al., *Laser Phys.*, **29**, 085701 (2019).
18. A. Kh. Kuptsov, I. A. Arutyunov, E. V. Zhmaeva, et al., *Prib. Tekh. Eksp.*, No. 4, 96-105 (2018).